



Ensuring Optimal Performance: Acceptance Testing of the Symbia Intevo Bold SPECT/CT System at SQCCRC, University Medical City, Muscat, Oman

S Kheruka*; N Al-Maymani; N Al-Makhmari; H Al-Saidi; S Al-Rashdi; A Al-Balushi; Tasnim Raii; V Jayakrishnan; A Jain; K Al-Riyami; R Al-Sukaity

Department of Radiology & Nuclear Medicine, Sultan Qaboos Comprehensive Cancer Care, and Research Center (University Medical City), Muscat, Oman.

***Corresponding Author(s): Subhash Chand Kheruka**

Consultant -Medical Physics (NM), Department of Radiology & Nuclear Medicine, Sultan Qaboos Comprehensive Cancer Care and Research Center, Muscat, Oman.
Tel: +96879289837; Email: skheruka@gmail.com

Abstract

Aim: This prospective study reports the acceptance testing of the Symbia Intevo Bold SPECT/CT scanner (Siemens Healthineers), recently installed at SQCCRC, University Medical City, Muscat, Oman, before its clinical implementation.

Materials and Methods: The acceptance tests were performed using a Low Energy High Resolution (LEHR) collimator and Technetium-99m (Tc-99m) as the radioactive source, following the manufacturer's protocols. The tests included physical inspection, peaking and tuning, intrinsic and extrinsic uniformity calibration, intrinsic energy resolution, and planar spatial resolution without scatter. Key performance parameters were evaluated, such as Full-Width at Half-Maximum (FWHM), system sensitivity, and count rate performance.

Results: All critical acceptance tests, including intrinsic energy resolution, energy calibration (symmetric curve), and extrinsic uniformity with the LEHR collimator, met the required specifications. System sensitivity and count rate performance were within the expected ranges, confirming the system's readiness for clinical use.

Conclusion: The Symbia Intevo Bold SPECT/CT system passed all performance tests successfully. The acceptance testing validated the system's optimal performance following international standards, ensuring its suitability for clinical operations.

Received: Feb 05, 2025

Accepted: Feb 19, 2025

Published Online: Feb 26, 2025

Journal: Journal of Radiology and Medical Imaging

Publisher: MedDocs Publishers LLC

Online edition: <http://meddocsonline.org/>

Copyright: © Kheruka S (2025). This Article is distributed under the terms of Creative Commons Attribution 4.0 International License

Keywords: Symbia intevo bold; Tc-99m; LEHR collimator; Acceptance testing; SPECT/CT; Spatial resolution; System sensitivity.

Cite this article: Kheruka SC, Maymani N, Makhmari N, Saidi H, Rashdi S, et al. Ensuring Optimal Performance: Acceptance Testing of the Symbia Intevo Bold SPECT/CT System at SQCCRC, University Medical City, Muscat, Oman. J Radiol Med Imaging. 2025; 8(1): 1099.



Introduction

The gamma camera is among the most widely utilized instruments in nuclear medicine for evaluating physiological function and diagnosing a range of pathologies. It plays a crucial role in imaging the bio-distribution of radiopharmaceuticals through dynamic and static studies of biological tissues [1,2]. This technology enables healthcare providers to capture functional images by detecting gamma radiation emitted from radiotracers, making it highly effective in identifying abnormalities such as cancer, cardiovascular diseases, and skeletal disorders.

One of the significant strengths of gamma cameras lies in their ability to integrate functional imaging with anatomical details obtained from X-ray or CT scans. This fusion of imaging modalities provides a comprehensive view of the patient's condition [3]. For instance, Single-Photon Emission Computed Tomography (SPECT), an enhancement of gamma camera functionality, enables precise three-dimensional localization of diseases, leading to more accurate diagnoses [4].

The recent installation of the Symbia Intevo Bold SPECT/CT system at the Sultan Qaboos Comprehensive Cancer Care & Research Center (SQCCRC) signifies a major milestone in the advancement of nuclear medicine in Oman. This achievement underscores the region's commitment to improving diagnostic capabilities and integrating cutting-edge technology into its healthcare infrastructure.

The performance of gamma cameras, however, can vary based on several factors, including the type of detector crystal used. The most commonly utilized materials for these detectors are hygroscopic Sodium Iodide (NaI) crystals, though newer technologies such as Cadmium-Zinc-Telluride (CZT) crystals offer improved performance [5,6]. Environmental conditions, such as temperature and humidity, can also significantly impact the functionality of gamma cameras [7]. Therefore, ensuring consistent image quality and minimizing patient radiation exposure necessitates rigorous quality assurance, including regular calibration and performance evaluations [8,9].

Acceptance testing forms a vital component of this quality assurance process. It provides baseline performance data to confirm that the equipment meets safety standards, performance benchmarks, and manufacturer specifications [10-12]. Routine acceptance tests for dual-head SPECT gamma cameras typically include evaluations of planar and rotational uniformity, spatial resolution, and the Center of Rotation (COR)—all of which are essential for maintaining image quality and diagnostic accuracy [13,14]. Previous studies have extensively documented the protocols and benefits of gamma camera acceptance testing [15,16].

By assessing critical parameters such as uniformity, resolution, and sensitivity, gamma cameras continue to serve as indispensable tools in nuclear medicine, delivering high-quality diagnostic images that support effective patient care and treatment planning [17-21].

Material & methods

The installation and commissioning of the Dual-Head SPECT Gamma Camera (Symbia Intevo Bold), with a standard 3/8" thick NaI crystal head, has been finalised at the Sultan Qaboos Comprehensive Cancer Care & Research Centre (SQCCRC). The gamma camera has detector size with a Field of View (FOV) of 53.3×38.7 cm, allowing high-quality imaging and excellent coverage for diverse diagnostic requirements.

This sophisticated device accommodates an energy spectrum from 35 to 588 keV, making it appropriate for many nuclear medicine applications. The gamma camera offers several acquisition modes, such as static, dynamic, gated, SPECT, gated SPECT, dynamic SPECT, whole-body, whole-body SPECT, SPECT/CT, and xSPECT, so ensuring versatile diagnostic capabilities. Quantitative accuracy assessments revealed a variation of <5%, guaranteeing exact imaging results. The tests were conducted in accordance with NEMA guidelines (NEMA NU 1-2012).

This work used the Low Energy High Resolution (LEHR) collimator to undertake critical assessments to guarantee maximum imaging efficacy with low-energy photon-emitting radionuclides, including Technetium-99m (Tc-99m). The uniformity test was conducted using Tc-99m and Co-57 to evaluate the detector's response constancy over the whole field of view, therefore reducing artefacts and enhancing dependability.

The spatial resolution test evaluated the system's capacity to discern tiny features by analyzing the Full Width at Half-Maximum (FWHM) of point sources, therefore validating the accuracy necessary for high-quality imaging. The sensitivity study focused on the system's efficacy in detecting gamma radiation. This assessment guaranteed precise photon detection from Tc-99m, enhancing patient dosage and picture fidelity.

The examination of energy resolution measured the system's capacity to distinguish photon energies, hence reducing scatter and improving clarity. The linearity testing confirmed that the system maintained spatial precision over the whole detector, guaranteeing that images were devoid of distortion.

The tests, performed with the suitable collimator, validated the system's capacity to provide precise, high-resolution diagnostic images. Upon completion of the acceptance testing, the surfaces of the tables and stands were decontaminated. The gamma camera underwent motion and axial calibrations, followed by energy calibration and automatic tuning of the detectors.

Acceptance testing and annual survey guidelines for dual-head SPECT gamma camera systems:

Acceptance testing and annual surveys for Dual-Head SPECT Gamma Camera systems must thoroughly inspect the system's physical condition, shielding integrity, safety interlocks, and the basic functionality of its associated computers and monitors. It is crucial to document all findings in a comprehensive report.

Physical inspection

Equipment condition assessment

A detailed physical inspection of the camera and all related components was performed. The inspection focused on identifying any visible defects such as scratches, cracks, or loose parts that might compromise system functionality. All filters were checked to ensure they were free of clogs or leaks, which could affect the imaging quality or system safety. The external surfaces of the camera were inspected for cleanliness and the absence of contamination.

Collimator mounting and integrity

The installed Low Energy High Resolution (LEHR) collimators were thoroughly examined to verify they were correctly mounted and securely fastened. This included ensuring that the collimators could be easily switched when necessary. Proper alignment and mechanical integrity of the collimators are essential

for ensuring that the imaging system maintains its precision and does not produce artifacts or distortions.

Detector movement and table functionality

The detector movement and table motion were tested to ensure smooth operation without any abnormal sounds, hesitations, or mechanical issues. The axial movement of the camera and table was observed to ensure accurate positioning during patient scans. Proper movement of these components is critical to obtaining clear, artifact-free images during both static and dynamic studies.

Control panel and positioning lights

The functionality of the control panel and the light markers, which guide patient positioning, were tested. All switches and indicators were verified to be responsive and operational. This ensures that operators can accurately position patients and perform diagnostic procedures without errors related to improper system function.

Safety systems and interlocks

Emergency stop and collision sensors

Safety systems, including emergency stop buttons and collision sensors, were rigorously tested to ensure that they function correctly. The emergency stop buttons, when pressed, should immediately halt all camera operations, safeguarding both the patient and the operator in the event of a malfunction. Additionally, collision sensors, particularly those on movable components such as the collimator, were tested to detect any contact and stop motion automatically, preventing potential injuries or equipment damage.

Radiation and room safety checks

Radiation warning lights and other room safety indicators were checked for visibility and functionality. These lights alert staff to radiation use, ensuring that proper protective measures are taken. Warning signs were inspected to verify that they were clearly displayed and appropriately located. The room door closure was tested to ensure it properly seals the room during imaging, maintaining a controlled environment and minimizing radiation exposure to those outside.

Personal protective devices

The availability and condition of personal protective devices, such as lead aprons, were verified. These devices are critical for protecting operators from radiation exposure during gamma camera procedures. The operator's ability to view the patient from the control room window was also confirmed, ensuring unobstructed supervision during scans.

Shielding integrity and radiation protection

Detector shielding inspection

An important part of the installation process involved testing the shielding integrity of the detector. Following NEMA guidelines, a leak scan was performed around the detector using a small radionuclide source (~1 mCi of ^{99m}Tc). This test involved moving the source around the detector and observing the count rates to identify any potential radiation leaks. Special attention was paid to the collimator interface to ensure that there were no radiation escapes at the point where the collimator meets the detector. Proper shielding is essential for both patient and operator safety.

Camera shielding and safety

The overall camera shielding was inspected to detect any potential weak points or damage that could lead to radiation leakage. Maintaining the integrity of the camera's shielding ensures that no unintended radiation exposure occurs, providing a safe environment for patients and healthcare workers. Any shielding defects were identified and scheduled for immediate correction.

System functionality and calibration

Image header information

The system's ability to correctly capture and display patient information within the image headers was verified. This includes details such as patient identification, date, and time of the scan. Accurate recording of this information is critical for proper patient record-keeping and traceability in diagnostic procedures.

Motion and axial calibration

The calibration of the camera's motion and axial alignment was performed to ensure that the system could move smoothly and accurately during imaging. This process helps confirm that the gamma camera can maintain precise positioning throughout the scan, ensuring the integrity of both static and dynamic images. Additionally, energy calibration was carried out to fine-tune the camera's energy detection settings, ensuring accurate and consistent imaging results.

Intrinsic and extrinsic calibration and verification

Preparation of the Tc-99m point source

To carry out intrinsic calibration and verification for the gamma camera, we prepared a Tc-99m point source with precise steps. First, a small piece of cotton was carefully placed into the cone portion of a vial, which would absorb the radiotracer. Then, the recommended activity of 35 μCi of Tc-99m was carefully dropped onto the cotton. This was used for both intrinsic calibration and verification procedures. Special attention was paid to avoid oversaturating the cotton or overfilling the vial to prevent any spillage or splashing of the radioactive material onto the vial's sides, which could compromise the procedure. Once the Tc-99m point source was properly prepared, it was ready for the calibration and verification processes to ensure that the gamma camera's detectors were operating with the required accuracy.

Utilization of the integrated source holder

Once prepared, the Tc-99m point source was placed into the integrated source holder, which is a retractable rod located at the foot end of the patient bed. The source holder was manually pulled out from its storage position to perform the necessary quality control tasks. The vial containing the point source was inserted into the end of the holder to accurately position the source for intrinsic calibration and verification. After the procedures were completed, the source holder was returned to the bed for secure storage. This system allowed for both accurate and efficient positioning of the point source, ensuring reliable quality control checks for the gamma camera's intrinsic performance.

Extrinsic calibration and verification setup

For extrinsic flood verification and calibration, a Co-57 sheet

source was used. The process began by positioning the sheet source holder on the patient bed, close to the pallet handle, to facilitate the calibration procedure. Once the system was homed, the patient pad was removed from the pallet to allow space for the source holder. The sheet source holder was then securely fastened to the pallet using hook-and-loop fasteners, with the base's pins fitting into the tracks on both sides of the pallet to ensure stability during the calibration process. The Co-57 sheet source was carefully centered within the holder's designated source area, ensuring precise alignment for accurate calibration and verification. This setup provided precise extrinsic calibration, crucial for maintaining the gamma camera's system performance during clinical imaging.

Methods for intrinsic spatial resolution and linearity testing

Spatial resolution testing

To evaluate the intrinsic spatial resolution of the gamma camera, a Co-57 flood source with an activity of 5 mCi was used in combination with a quadrant bar phantom. This process was designed to test the system's ability to distinguish fine details along both the X and Y axes of the detector. The quadrant bar phantom was carefully placed in front of the gamma camera, ensuring proper alignment with the detector. The camera's zoom and image matrix settings were adjusted so that the pixel size perpendicular to the bar pattern was less than 0.2 Full Width at Half Maximum (FWHM). During the test, a minimum of 250 counts per pixel was acquired at the peak locations of the bar images to guarantee accurate spatial resolution data. This method allowed for a precise evaluation of the camera's ability to capture detailed images without distortion.

Linearity testing

Linearity testing was then conducted to determine the system's ability to detect straight lines without introducing distortions. The Line-Spread Functions (LSFs) were obtained by applying a 30 mm wide profile across each bar image, and at least 1500 counts were collected at the peak. This provided robust data for evaluating the system's linearity. In instances where the pixel size exceeded 0.2 FWHM, a parabolic fit was applied to the three highest values, and linear interpolation was used to determine the half-maximum points, ensuring a more accurate measurement of the bar spacing and image clarity. During the test, the bar images were also visually inspected for any signs of nonlinearity, such as bending or distortions, which could indicate tube balance issues. Nonlinearity was classified based on the severity of the distortion: none, just noticeable (less than 1 mm), or significant (greater than 1 mm).

Recording spatial resolution and smallest detectable bar size

After completing the tests, the Full Width at Half Maximum (FWHM) was recorded for each image. For the quadrant bar phantom, the smallest resolvable bar size was multiplied by 1.75 to determine the smallest detectable bar size. This value reflected the gamma camera's ability to resolve the finest details, which is a critical measure of its overall imaging precision.

Extrinsic planar spatial resolution

The spatial resolution and linearity of the gamma camera were evaluated using a bar phantom, a 5-10 mCi Co-57 flood sheet source, and line sources with an activity of 2-3 mCi (74-111 MBq). The acquisition process was continued until a cumulative total of 5 million counts was obtained for each image to ensure sufficient data collection.

To assess spatial resolution, the Co-57 source was positioned above the bar phantom on the collimator's face, utilizing the Low Energy High Resolution (LEHR) collimator. For optimal resolution, the maximum matrix size of 1024×1024 was selected, with pixel widths less than half the width of the narrowest bars in the phantom. The acquisition process persisted until 5 million counts per image were reached, which provided high-quality data for further analysis.

Line-Spread Functions (LSFs) were generated by applying broad profiles over the bar images. A parabolic fit was applied to the three highest count values at the apex of the LSF, followed by linear interpolation to determine the half-maximum locations. The smallest identifiable bar size was determined visually, ensuring that at least 50% of the bar length was clearly visible in at least one quadrant of the image. To evaluate spatial linearity, the bar images were examined for any signs of bending or distortion, which could indicate issues such as gamma camera tube imbalance.

The Full Width at Half Maximum (FWHM) was calculated by multiplying 1.75 by the smallest bar size that could be identified by the gamma camera. FWHM values were documented for Tc-99m and other radionuclide/collimator combinations, as well as the minimum resolvable bar size for Co-57 and any observed nonlinearity during the process.

The rectangular bar phantom used in this study contained four quadrants with bar widths of 2.0 mm, 2.5 mm, 3.0 mm, and 3.5 mm. The Co-57 flood sheet source was utilized to generate the images necessary for evaluating spatial resolution and linearity.

For the line-source measurements, sources with an activity of 2-3 mCi (74-111 MBq) were placed parallel to and 10 cm from the collimator face, positioned perpendicular to the measurement axis. Images were captured along both the X-axis and Y-axis. The matrix dimensions for this part of the study were set to 128×128, with a magnification factor of 1. As with the planar spatial resolution test, each acquisition continued until 5 million counts were obtained, ensuring a sufficient dataset for analysis.

At the computer workstation, Line-Spread Functions (LSFs) were generated by applying a broad profile (typically 30 mm) over each line-source image along both the X and Y directions. A parabolic fit was applied to the three highest count values at the peak of the LSF, followed by linear interpolation to locate the half-maximum positions on both sides of the peak. This method provided accurate spatial resolution data for further examination.

Analysis of spatial linearity

The analysis of spatial linearity involved determining whether the images of the line source or bar pattern appeared straight without any visible distortions. Any bending in the bars, especially near a Photomultiplier Tube (PMT), could indicate a loss of tube balance or issues with the detector's performance. Based on visual inspection, spatial linearity was classified as follows:

No observable nonlinearity: The bars or line sources appeared perfectly straight, indicating optimal spatial linearity and proper detector performance.

Just noticeable nonlinearity: Minor deviations, typically less than 1 mm, were present, though they did not significantly affect the image quality.

Significant nonlinearity: Distortions greater than 1 mm were detected, suggesting potential issues with the gamma camera that may require correction.

Since spatial linearity is not directly displayed in millimeters (mm), the degree of displacement was calculated based on the pixel size of the image. This enabled accurate determination of any observed displacements or distortions, providing a clear assessment of the system's performance in maintaining spatial accuracy.

Method for evaluating energy resolution

Prepare the detector

To evaluate energy resolution, the first step is to prepare the detector. This involves removing the collimator from the detector head and ensuring that the detector is properly aligned with the source to allow for accurate energy measurements. Without the collimator, the detector is exposed directly to the source, enabling a clear energy spectrum to be acquired.

Position the lead mask

Next, a lead mask is centrally placed on the crystal housing to shield the unused areas of the detector. This ensures that the radiation is focused only on the detector's active area, minimizing any interference from surrounding areas. The lead mask helps to concentrate the radiation exposure, making the energy measurement more precise.

Mount the 99mTc source

For this evaluation, a 99mTc source with an activity of 600 μ Ci is used. The source is positioned at five times the maximum Useful Field of View (UFOV) from the detector's central axis, following the manufacturer's guidelines. This distance is crucial to ensure uniform radiation exposure across the detector's active surface, which is important for an accurate energy resolution test.

Center the PHA window

The Pulse Height Analyzer (PHA) window must be adjusted to center on the 20% photopeak for 99 mTc. The energy peak for 99 mTc is typically 140 keV, and the window should be set accordingly based on the manufacturer's recommended default settings. Properly centering the PHA window ensures that the energy spectrum is captured around the desired peak for analysis.

Acquire the spectrum

Once the PHA window is centered, the energy spectrum is acquired. The process continues until a clear photopeak is visible on the spectrum display. This photopeak is essential for assessing the energy resolution, as it represents the detector's ability to distinguish between different gamma photon energies.

Visual estimation of FWHM

After acquiring the spectrum, the next step is to visually estimate the Full Width at Half Maximum (FWHM) of the photopeak. The FWHM represents the width of the photopeak at half of its maximum height and is a critical parameter in determining energy resolution. By adjusting the energy window, the FWHM can be observed and estimated directly from the spectrum.

Calculate energy resolution

The final step in the process is to calculate the energy resolution using equation (1). This formula provides the percentage of

energy resolution, which is an important performance indicator for the gamma camera system.

$$\text{Energy Resolution (\%)} = \frac{\text{FWHM of the photopeak}}{\text{Mean energy (140 keV)}} \times 100 \quad (1)$$

A lower energy resolution percentage indicates better system performance, as it reflects the camera's ability to clearly distinguish between different photon energies, minimizing noise and scatter.

Method for evaluating tomographic spatial resolution

Position the line source

To begin the evaluation of tomographic spatial resolution, position the line source containing 99mTc (1 mCi/cm³) parallel and as close as possible to the Axis of Rotation (AOR). Proper alignment with the AOR ensures accurate measurements during the scan and reliable results.

Set the radius of rotation (ROR)

Set the detectors to a Radius of Rotation (ROR) of 20 cm. If this is not feasible, use the smallest possible ROR and record the value. Maintaining a consistent ROR across all acquisitions is crucial for ensuring accuracy in the spatial resolution evaluation.

SPECT acquisition

Acquisition settings: Use a circular orbit with step-and-shoot mode to capture the projection images. Select a matrix size of 128x128 with 128 (or 120) views over 360°. If necessary, apply a zoom to achieve a pixel size between 3.0 and 3.5 mm. Ensure the acquisition time per stop is sufficient to capture at least 100,000 counts in the first image. These settings will allow for high-quality data acquisition.

SPECT image reconstruction

Reconstruct the data: Reconstruct the SPECT data using Filtered Back Projection (FBP) with a ramp filter. Alternatively, if using an iterative reconstruction method, make sure to disable any resolution-enhancement features. This step ensures the natural spatial resolution of the system is accurately represented in the results.

Planar image acquisition

Acquire the planar image: After completing the SPECT acquisition, acquire a planar image without adjusting the line source. Use the same Radius of Rotation (ROR), matrix size, and zoom settings as in the SPECT acquisition. Collect at least 100,000 counts per image to ensure a proper comparison between the planar and tomographic spatial resolutions.

Image processing and analysis

Analyze reconstructed images: In the reconstructed axial images, the line source will appear as point-source distributions. Measure the Full Width at Half Maximum (FWHM) of the Point-Spread Functions (PSFs) by drawing count-density profiles across the point sources. This measurement will help assess the detector's ability to distinguish fine image details.

Analyze key slices: Focus on three transaxial slices: one in the middle of the line source and two slices about 1 cm from each end. For each slice, draw a 1-pixel-wide profile through the hottest pixel in both the X and Y directions. Use linear interpolation to calculate the FWHM for each slice, which will provide

insight into the spatial resolution.

Record the FWHM: Record the FWHM values in millimeters for all PSFs in the axial slices. Then, in the planar images, measure the FWHM at the same three slice locations. Calculate the average FWHM across both the planar and tomographic data to compare the two spatial resolutions.

Compare spatial resolutions

Compare the average spatial resolutions: Compare the average tomographic spatial resolution to the average planar spatial resolution. If the tomographic resolution exceeds the planar resolution by more than 10%, investigate potential causes such as errors in the Center of Rotation (COR), Multiple Head Registration (MHR), or detector head-tilt. Identifying and correcting these issues is essential for maintaining system accuracy and performance.

Method for evaluating extrinsic planar sensitivity

Position the sensitivity source

To evaluate the extrinsic planar sensitivity of the gamma camera, place the sensitivity source (containing 20-80 MBq of ^{99m}Tc in 2-3 ml of water) in a 150 mm diameter flat plastic dish. The source must be centered over the Useful Field of View (UFOV) of the gamma camera's detector, ensuring it is placed 10 cm away from the detector surface. This specific distance must be maintained for all measurements to ensure consistency.

Use of a source holder

Use a low-attenuating holder, such as a thin cardboard box, to keep the source positioned correctly at the specified distance from the collimator. This ensures minimal scatter or attenuation, which could affect the accuracy of the sensitivity measurement.

Setup of the detector

For the detector setup, select the low-energy parallel-hole collimator routinely used in clinical practice. If the gamma camera is part of a multi-detector system, perform the sensitivity test for each detector individually to evaluate each detector's performance.

Acquisition settings

The matrix size for acquisition is not critical for this test, so a standard matrix size can be used. Set the acquisition time to at least 1 minute to ensure that sufficient data is collected for an accurate sensitivity measurement.

Background subtraction

After measuring the sensitivity of the source, remove the source and immediately acquire a background image for 1 minute. This helps subtract the background counts from the sensitivity calculation. Be sure to record both the time of the assay and the time of imaging to apply any required decay corrections.

Perform sensitivity test for all detectors

Repeat the sensitivity measurement for each detector, radionuclide, and collimator combination used in your facility. This ensures that sensitivity is accurately measured across all system components.

Total counts calculation

After the images are acquired, calculate the total counts for

both the source and background images using the full image matrix for each detector, radionuclide, and collimator combination. For multi-detector systems, calculate the sensitivity ratio by comparing the total counts for each detector.

Sensitivity calculation

Finally, subtract the background counts from the total source counts for each detector. Calculate the sensitivity in units of counts per minute per unit activity (CPM/kBq or CPM/ μCi). This provides the system's sensitivity value, reflecting how effectively each detector captures gamma radiation.

Method for testing maximum count rate of a scintillation camera

Remove the collimator

To begin testing the maximum count rate of the scintillation camera, start by removing the collimator from the detector head. This prepares the system for direct detection. Ensure that the detector head is positioned horizontally to maintain proper alignment during the test.

Position the lead mask

Place a lead mask centrally on the crystal housing of the detector. This ensures that scatter is minimized, and the radiation is focused directly on the central part of the detector. The lead mask plays an important role in concentrating the radiation for accurate measurements.

Set the PHA window

Next, center the manufacturer's default Pulse Height Analyzer (PHA) window on the photopeak of ^{99m}Tc . This step is crucial for ensuring the measurement is accurately aligned with the radionuclide's energy peak, resulting in reliable count data.

Mount the point source

Mount a point source containing approximately 4 MBq (100-500 mCi) of ^{99m}Tc onto a movable stand. Position the source on the central axis of the detector head, ensuring that there are no nearby objects that could cause radiation scatter and interfere with the accuracy of the measurement. This positioning allows the system to detect the source efficiently.

Measure and record the count rate

Gradually move the source closer to the detector, carefully monitoring the count rate as the distance decreases. As the source approaches the detector, the count rate will increase until it reaches a maximum point. Afterward, the count rate will decrease as the system becomes saturated. Record the maximum count rate observed when it peaks, as this represents the maximum count rate capability of the scintillation camera.

Reassemble the system

Once the test is complete, remove the point source, the movable stand, and the lead mask. Finally, replace the collimator on the detector head to restore the system to its normal operational configuration. This ensures the camera is ready for standard clinical use after the testing procedure.

This procedure is designed to effectively determine the maximum count rate of the scintillation camera, verifying that the system is operating within its expected performance limits.

Method for testing center of rotation (COR) offset and multiple head registration (MHR)

Purpose

The purpose of this procedure is to test and verify the Center of Rotation (COR) offset, alignment of the camera Y-axis, and head tilt relative to the axis of rotation in a SPECT system. This test is essential when there is an error in the resolution in air test and serves as an extended version of the procedure outlined in the manufacturer's SPECT system manual.

Frequency

This test should be performed monthly or as recommended by the manufacturer to ensure consistent system performance.

Calibration of COR and MHR

The calibration of both the COR and MHR is typically done simultaneously during a single measurement. It's important to follow the exact procedure provided in the manufacturer's manual specific to your SPECT system. In some systems, separate measurements are required for both the 180° and 90° detector configurations. The 90-degree configuration is commonly used for cardiac SPECT imaging.

Setting up the point sources

To begin, place point sources either on the imaging table or in a specially designed fixture that ensures proper alignment. The SPECT acquisition should involve a full 360° rotation of each detector head around these point sources. Correct positioning of the sources is crucial for accurate calibration.

SPECT acquisition

Acquire projection images from the 360° rotation for each detector head. The calibration software will then identify the projected location of each point source in the sinogram and track its position as a function of the detector angle. This data allows the system to calculate both COR and MHR without the need for a full tomographic reconstruction.

Detecting head tilt

Axial head tilt is not visible in the sinogram, but it can be detected by reviewing a cine display of the projection images. If there is a sinusoidal oscillation in the axial (vertical) direction of the projections, this indicates the presence of head tilt. Unlike COR and MHR, there is no calibration procedure for correcting head tilt; instead, it requires mechanical adjustment by a service engineer.

Projection image processing and analysis

Most manufacturers provide software that automatically calculates corrections needed for COR and MHR and incorporates these corrections into the standard tomographic acquisition and reconstruction processes. The methods of analysis may vary depending on the manufacturer, so it is essential to follow the manufacturer's guidelines for each specific system.

Tolerance & reference values

The mean value of the center of rotation offset should be less than 2 mm. If the offset exceeds this threshold, a correction must be applied to the system.

The COR offset should remain consistent across both the center and edges of the field of view, with all measurements

falling within 2 mm of each other.

For multi-head systems, the Y=0 axis position and the Y gain should match between both detector heads, ensuring proper alignment across the system.

This process helps ensure that the SPECT system operates correctly, maintaining accuracy in image acquisition and reducing the risk of misalignment during clinical imaging. Regular testing and verification of COR and MHR are essential for achieving high-quality, reliable imaging results, which are critical for accurate patient diagnosis and treatment planning.

Results

Peaking & Tuning

This section outlines the results of the Peaking & Tuning test using a Tc-99m Point Source with an activity of 1 MBq. The data is provided for both Detector 1 and Detector 2, with a comparison to the specifications and an accompanying note.

Dead Time %: Both detectors fall within the **3-9%** specification range, indicating that the system is operating optimally without significant data loss due to dead time.

Peak Shift: The peak shifts for **Detector 1** and **Detector 2** are well within the acceptable **±3.0** range, with minimal deviation observed (-0.01 and -0.09, respectively), indicating stable energy alignment as shown in Table 14.1

14.1 Tc-99m Point Source (Activity: 1 MBq)

Parameter	Detector 1	Detector 2	Specification	Note
Dead Time %	8.25	8.5	3-9	P
Peak Shift	-0.01	-0.09	± 3.0	P

Tuning: Both **Detector 1** and **Detector 2** were successfully **tuned** to the required specifications, confirming that the system is calibrated for accurate performance as shown in Table 14.2.

14.2 Tc-99m Point Source Calibration (Activity: 1 MBq)

Parameter	Detector 1	Detector 2	Specification	Note
Tuning	Tuned	Tuned	N/A	P

Intrinsic and extrinsic uniformity

Intrinsic uniformity

The intrinsic uniformity results for both detectors during the calibration process demonstrate that both integral and differential uniformity fall within the manufacturer's specifications for the Central Field of View (CFOV) and Useful Field of View (UFOV).

For Detector 1, the integral uniformity was 1.17% (CFOV) and 1.39% (UFOV), while the differential uniformity measured 0.65% (CFOV) and 0.91% (UFOV).

For Detector 2, the integral uniformity was 1.37% (CFOV) and 1.45% (UFOV), with differential uniformity values of 1.04% (CFOV) and 1.04% (UFOV).

All values were within the specified limits of 2.9% (CFOV) and 3.7% (UFOV) for integral uniformity, 2.5% (CFOV), and 2.7% (UFOV) for differential uniformity, indicating that the system passed the uniformity calibration test.

Intrinsic uniformity (Verification)

In the verification phase, the integral and differential uniformity remained within the acceptable ranges:

Detector 1 showed integral uniformity of 3.41% (CFOV) and 4.44% (UFOV), while differential uniformity was 1.74% (CFOV) and 2.22% (UFOV).

Detector 2 exhibited integral uniformity of 4.04% (CFOV) and 4.94% (UFOV), with differential uniformity of 1.94% (CFOV) and 2.21% (UFOV).

16.3. Impression

These values are within the specifications of 5% (CFOV) and 6% (UFOV) for integral uniformity and 2.5% (CFOV) and 3% (UFOV) for differential uniformity, confirming the detectors' stable and reliable performance during the verification process.

PMT gain and uniformity assessment

PMT gain adjustment is crucial for achieving consistent uniformity and ensuring high-quality imaging in gamma cameras. Imbalances in PMT gain can lead to artifacts and non-uniformity, compromising diagnostic accuracy. Figure 1 illustrates how PMT gain adjustments affect uniformity tests and their correlation with imaging artifacts.

- **Figure 1A:** Shows the uniformity test performed using Tc-99m, demonstrating excellent uniformity with no visible artifacts.
- **Figure 1B:** Depicts the uniformity test performed using I-131, where noticeable "hot spot" defects are present. These defects were traced back to excessively high gain in specific PMTs, as illustrated in **Figure 1E**.
- **Figure 1C:** Displays the uniformity test performed using I-131 after recalibrating the PMT gain to the normal range, as seen in **Figure 1F**. This adjustment eliminated the hot spot artifacts, restoring uniformity and achieving diagnostic-quality imaging.
- **Figure 1E and Figure 1F** provide a detailed view of PMT gain calibration:
- **Figure 1E:** Shows the PMT gain status before adjustment, where some PMTs were operating at excessively high gain levels. This imbalance directly caused the hot spots observed in **Figure 1B**.
- **Figure 1F:** Illustrates the PMT gain after recalibration, with all PMTs adjusted to the normal range. This correction resulted in the improved uniformity seen in **Figure 1C**.

Additionally, **Figure 1D** presents a thyroid scan performed using I-131. The scan exhibits a defect caused by a "hot spot" artifact, which directly correlates with the non-uniformity seen in **Figure 1B**. This highlights how improper PMT gain calibration can affect diagnostic imaging by introducing artifacts that obscure or mimic pathology.

This example underscores the importance of regular PMT gain evaluations and adjustments to maintain uniformity across radionuclides, eliminate artifacts, and ensure consistent, high-quality diagnostic imaging.

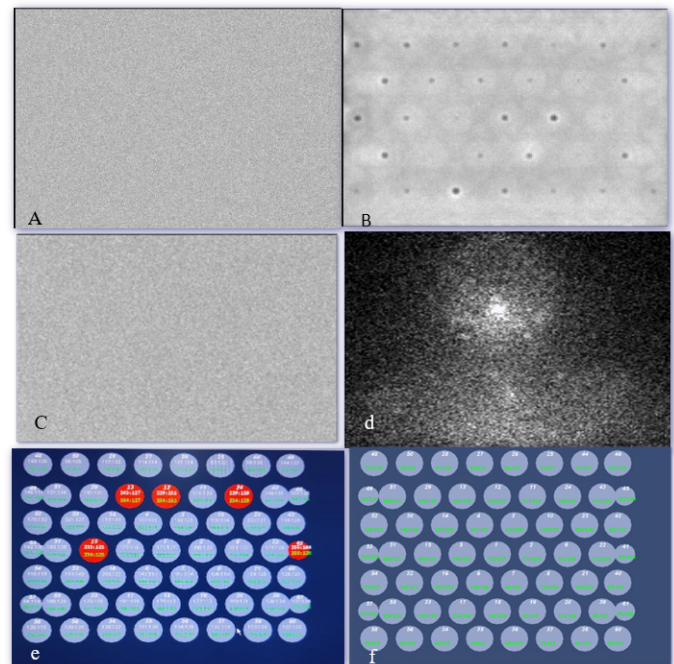


Figure 1: Impact of PMT Gain on Uniformity and Imaging: The figure demonstrates how PMT gain affects uniformity and image quality. (A) shows excellent uniformity with Tc-99m under optimal gain, while (B) highlights hot spot defects with I-131 due to high PMT gain (E). After recalibration to normal levels (F), uniformity is restored, as shown in (C). (D) depicts a thyroid scan with defects caused by the non-uniformity in (B) underscoring the need for proper PMT gain calibration.

Extrinsic uniformity

The extrinsic uniformity test was conducted using a Co-57 flood source for both the calibration and verification phases. The values obtained for Detector 1 and Detector 2 were well within the manufacturer's specified limits.

Calibration Results (Co-57 Flood Source)

During calibration, both integral and differential uniformity results for the Central Field of View (CFOV) and the Useful Field of View (UFOV) were within acceptable ranges:

Detector 1 recorded an integral uniformity of 1.90% for CFOV and 3.42% for UFOV. The differential uniformity was 1.05% (CFOV) and 1.51% (UFOV).

Detector 2 showed an integral uniformity of 2.56% (CFOV) and 4.95% (UFOV), while the differential uniformity was 1.21% (CFOV) and 1.40% (UFOV).

Both detectors performed within the manufacturer's specifications of 5% for CFOV and UFOV (integral and differential), indicating that the system met the calibration standards.

Verification results (Co-57 flood source)

In the verification phase, the extrinsic uniformity continued to meet the required specifications:

Detector 1 had an integral uniformity of 2.64% for CFOV and 2.83% for UFOV. The differential uniformity was 1.85% (CFOV) and 2.68% (UFOV).

Detector 2 recorded an integral uniformity of 2.71% for CFOV and 2.96% for UFOV, with a differential uniformity of 2.42% for both CFOV and UFOV.

Both detectors were within the specification limits of 5% for integral and differential uniformity, confirming that they passed the verification test.

Impression

The results of the extrinsic uniformity test using the Co-57 flood source demonstrate that both detectors performed well within the manufacturer's specifications. Detector 1 showed values of 2.64% (CFOV) and 2.83% (UFOV) for integral uniformity during verification, while Detector 2 recorded 2.71% (CFOV) and 2.96% (UFOV). The differential uniformity values also remained within acceptable ranges. Both detectors consistently met the calibration and verification standards, ensuring reliable and accurate imaging performance.

Results

Intrinsic spatial resolution

The intrinsic planar spatial resolution was evaluated using a bar phantom and a Co-57 flood source. Both Detector 1 and Detector 2 resolved a minimum bar size of 3.20 mm, which meets the manufacturer's specification of ≤ 3.2 mm. This indicates that both detectors are functioning as expected in terms of resolving fine spatial details, ensuring that the system can capture high-quality images with precise resolution.

In addition to the bar size, the Full Width at Half Maximum (FWHM) was also measured for both detectors. The FWHM for Detector 1 and Detector 2 was 5.60 mm, which falls well within the acceptable limit of ≤ 7.5 mm. This further confirms that both detectors are maintaining the required spatial resolution performance.

Impression

The results of the intrinsic planar spatial resolution test demonstrate that both detectors are operating within the required specifications. The minimum resolvable bar size of 3.20 mm and the FWHM of 5.60 mm for both detectors indicate that the system can reliably capture images with high spatial accuracy. These results affirm that the system is functioning optimally in terms of intrinsic spatial resolution.

Extrinsic planar spatial resolution

The extrinsic planar spatial resolution was assessed using a bar phantom and a Co-57 flood source. Both Detector 1 and Detector 2 performed within the specified limits for spatial resolution.

For Detector 1, the minimum resolvable bar size was measured at 3.20 mm, which meets the required specification of ≤ 3.2 mm. Similarly, Detector 2 also resolved the minimum bar size at 3.20 mm, confirming that both detectors can resolve fine spatial details as per the system's specifications.

Additionally, the Full Width at Half Maximum (FWHM) was recorded at 5.60 mm for both detectors, well below the specification limit of ≤ 7.5 mm. This further demonstrates that both detectors perform with a high degree of spatial resolution, ensuring accurate and detailed image capture.

Impression

The results of the extrinsic planar spatial resolution test confirm that both Detector 1 and Detector 2 are operating within acceptable limits. With a minimum resolvable bar size of 3.20 mm and an FWHM of 5.60 mm for both detectors, the system

meets the required standards for extrinsic spatial resolution. These findings validate the system's capability to provide high-quality imaging with precise resolution, ensuring optimal performance in clinical settings.

Tomographic spatial resolution without scatter

The tomographic spatial resolution without scatter was tested using a Tc-99m line source with an activity of 40 MBq. The measurements were conducted with both detectors using two different reconstruction methods: Filtered Back Projection (FBP) and Flash 3D.

For both detectors, the Full Width at Half Maximum (FWHM) with FBP reconstruction was 9.65 mm, which is within the specified limit of ≤ 10.8 mm. This indicates that the system is performing adequately when using traditional FBP reconstruction.

When using Flash 3D reconstruction, the FWHM was significantly improved, with a value of 4.82 mm, again within the specified limit of ≤ 4.4 mm. Though slightly above the specification, the result still passed the test, confirming acceptable system performance with Flash 3D technology.

Impression

The results of the tomographic spatial resolution without scatter test demonstrate that both detectors performed well with the FWHM values meeting the required specifications. With FBP, the system achieved an FWHM of 9.65 mm, and with Flash 3D, the FWHM was 4.82 mm. These findings confirm that the system provides adequate spatial resolution for tomographic imaging, ensuring high-quality image reconstruction in clinical applications.

System planar sensitivity

The system planar sensitivity was tested using a Tc-99m source with an activity of 55 MBq placed in a Petri dish. The sensitivity was measured for both Detector 1 and Detector 2 at 10 cm from the detectors, using a Low Energy High Resolution (LEHR) collimator.

Both Detector 1 and Detector 2 showed a sensitivity of 126 CPS/MBq, which exceeds the specified requirement of ≥ 91 CPS/MBq. This confirms that both detectors meet the required sensitivity performance standards.

The detector variation percentage between Detector 1 and Detector 2 was minimal, at 0.01%, which is well within the specification limit of $< 5\%$. This indicates that there is negligible variation in sensitivity between the two detectors, ensuring consistent performance across the system.

Impression

The results of the system planar sensitivity test confirm that both Detector 1 and Detector 2 performed above the required specification, achieving 126 CPS/MBq for both detectors. The extremely low detector variation of 0.01% demonstrates consistent sensitivity between detectors, ensuring reliable and accurate imaging performance across the system.

Intrinsic count rate performance

The intrinsic count rate performance was evaluated using a Tc-99m source with an activity of 40 MBq placed in a syringe. The maximum count rate was measured for both Detector 1 and Detector 2.

Both Detector 1 and Detector 2 achieved a maximum count rate of 395 kps (kilo counts per second), which exceeds the specified requirement of ≥ 310 kps. This indicates that the system is capable of handling high count rates efficiently without experiencing significant count loss.

Impression

The results of the intrinsic count rate performance test confirm that both Detector 1 and Detector 2 exceeded the required specifications, achieving a maximum count rate of 395 kps. These results demonstrate that the system can operate effectively at high activity levels, ensuring reliable performance during clinical imaging.

Multiple head registration (MHR) and center of rotation (COR)

The **Multiple Head Registration (MHR)** and **Center of Rotation (COR)** tests were conducted using both **LEHR** and **MELP collimators** at **180 degrees** for **Detector 1** and **Detector 2**.

Collimator: LEHR 180 Degrees

Center of Rotation (COR):

Detector 1 measured **0.768 mm** and **Detector 2** measured **-0.075 mm**, both well within the specification of ≤ 10 mm.

Axial Shift:

Detector 1 showed an axial shift of **0.34 mm**, while **Detector 2** had an axial shift of **-0.34 mm**, both meeting the specification limit of ≤ 5 mm.

Back Projection Angle:

The back projection angles were **0.036°** for **Detector 1** and **-0.036°** for **Detector 2**, which are well within the specification of $\leq 0.8^\circ$.

System Resolution @ 20 cm:

The system resolution at **20 cm** was **16.39 mm** for **Detector 1** and **16.378 mm** for **Detector 2**, confirming consistent performance across both detectors.

Collimator: MELP @ 180 Degrees

Center of Rotation (COR):

Detector 1 had a COR of **1.037 mm**, while **Detector 2** recorded **-0.068 mm**, both falling within the ≤ 10 mm specification.

Axial Shift:

The axial shift was **0.3 mm** for **Detector 1** and **-0.3 mm** for **Detector 2**, both well within the limit of ≤ 5 mm.

Back Projection Angle:

The back projection angle for **Detector 1** was **-0.007°**, and for **Detector 2**, it was **0.007°**, which is within the $\leq 0.8^\circ$ specification.

System Resolution @ 20 cm:

The system resolution at **20 cm** for **Detector 1** was **23.821 mm**, and for **Detector 2**, it was **23.693 mm**, showing accurate and consistent system performance.

Impression

The results for Multiple Head Registration (MHR) and Center of Rotation (COR) demonstrate that both detectors performed well within the specified limits across all tested parameters. The measurements for COR, axial shift, and back projection angle for both LEHR and MELP collimators at 180 degrees met the required specifications, confirming the system's alignment and accuracy in head registration.

The successful validation of the system's parameters, including intrinsic and extrinsic uniformity, spatial resolution, and sensitivity, confirms its readiness for routine clinical operations, ensuring reliable diagnostic imaging.

Impact of faulty COR on cardiac imaging and correction

Figure 2 illustrates the effects of a faulty Center of Rotation (COR) on cardiac SPECT imaging at the 90° position and the improvement after recalibration.

The top row shows a distinct break in the sinogram (indicated by arrows), a decreased tracer activity area in the apical region, and a hot spot in the inferior wall of the myocardium. These artifacts were caused by a misaligned COR at the 90° position, leading to significant distortion in the cardiac image.

To address these defects, the COR was evaluated and corrected for both 90° and 180° positions. The bottom row displays the corrected cardiac SPECT imaging after proper calibration. The previously observed defects are resolved, with the image now showing a uniform, horseshoe-shaped myocardial tracer distribution, indicative of normal perfusion.

This figure emphasizes the necessity of performing COR calibration for both 90° and 180° positions to ensure accurate image reconstruction and eliminate artifacts that could lead to diagnostic errors.

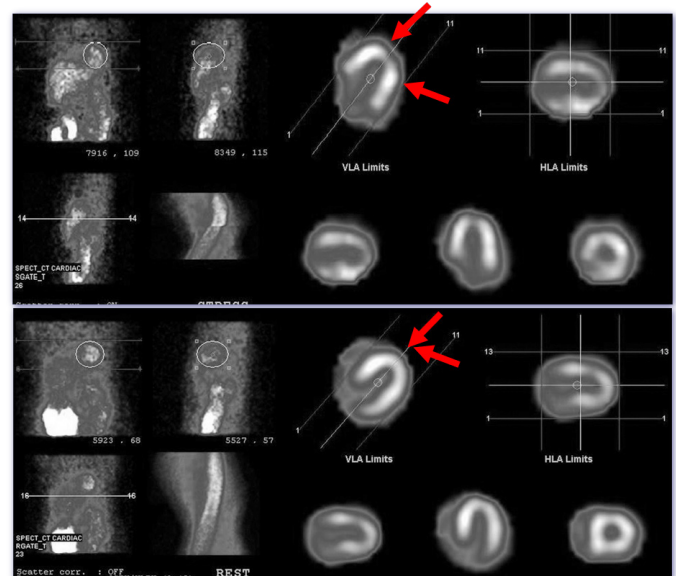


Figure 2: Effect of Faulty COR and Its Correction on Cardiac Imaging: The top row shows artifacts, including a break in the sinogram (arrows), decreased apical tracer activity, and a hot spot in the inferior wall, caused by faulty COR at 90°. After correcting the COR for both 90° and 180°, the bottom row displays a uniform, horseshoe-shaped myocardial tracer distribution, indicating normal perfusion.

Discussion

These results underscore the system's ability to deliver high-quality diagnostic images, critical for precise disease detection and treatment planning. By ensuring reliability and adherence to stringent performance standards, the Symbia Intevo Bold reinforces confidence in its clinical application. The results from the various tests conducted on the gamma camera system demonstrate that the system is operating well within the manufacturer's specifications and meeting performance expectations across all critical metrics. These tests, including intrinsic and extrinsic uniformity, spatial resolution, planar sensitivity, count rate performance, and Multiple Head Registration (MHR), confirm that the system is calibrated and functioning optimally, ensuring reliable and accurate imaging for clinical use.

Uniformity performance

The results for both intrinsic and extrinsic uniformity reveal that the system maintains high levels of consistency across the Central Field of View (CFOV) and Useful Field of View (UFOV). For intrinsic uniformity, both detectors displayed integral and differential uniformity values that were well within the specifications. This ensures that the detectors are producing images with uniform intensity, minimizing any artifacts or distortions that could affect image quality.

Similarly, the extrinsic uniformity test using the Co-57 flood source showed that the integral and differential uniformity for both detectors met the specified limits. The ability of the system to maintain extrinsic uniformity ensures that images taken in the presence of collimators and external sources maintain the same level of accuracy and reliability as intrinsic uniformity.

Spatial resolution

The spatial resolution results, both intrinsic and extrinsic, show that the system can resolve fine details. Both detectors resolved a minimum bar size of 3.20 mm, meeting the required specification of ≤ 3.2 mm, while the Full Width at Half Maximum (FWHM) measurements for both intrinsic and extrinsic spatial resolution were well within the acceptable range. These results confirm that the system can capture high-resolution images, which is crucial for detailed diagnostic imaging, ensuring that even small anatomical structures can be detected and analyzed.

Sensitivity and count rate performance

The system planar sensitivity results, measured using a Tc-99m source, showed that both detectors achieved sensitivity values of 126 CPS/MBq, which exceeded the minimum specification of ≥ 91 CPS/MBq. Additionally, the detector variation between the two detectors was negligible, at 0.01%, well below the allowed limit of $< 5\%$. This consistency in sensitivity across both detectors ensures uniform image quality and reliability across different imaging scenarios, particularly when detecting low-energy gamma emissions.

The intrinsic count rate performance further demonstrated the system's ability to handle high-activity sources, with both detectors achieving a maximum count rate of 395 kps, significantly exceeding the specification of ≥ 310 kps. This performance ensures that the system can handle high patient doses or activity levels without experiencing significant count loss, which is critical for dynamic studies or high-activity imaging.

Multiple head registration and center of rotation

The results from the Multiple Head Registration (MHR) and Center of Rotation (COR) tests indicate that the system maintains proper alignment between the two detector heads. For both the LEHR and MELP collimators at 180 degrees, the center of rotation measurements was well within the specified limit of ≤ 10 mm, with minimal axial shift and back projection angle errors. This alignment is crucial for SPECT imaging, where accurate registration between the detectors is necessary to create precise tomographic images. The consistent performance across both detectors ensures that the system can provide high-quality reconstructions with minimal distortion.

Overall system performance

Overall, the gamma camera system has demonstrated strong performance across all test categories. The system's ability to maintain uniformity, sensitivity, spatial resolution, and proper head alignment ensures that it is well-calibrated for routine clinical use. These results are critical in confirming the system's reliability in producing diagnostic-quality images, which is essential for accurate patient diagnosis and treatment planning.

The fact that the system performed within or exceeded the required specifications across all tested parameters reflects its robustness and reliability. Regular testing and maintenance, such as the ones performed in these evaluations, are essential for ensuring the continued high performance of the system, which in turn supports accurate and reliable patient care in nuclear medicine.

Conclusion

This research confirms the performance of the Symbia Intevo Bold system and develops a framework for implementing comparable breakthroughs in nuclear medicine inside developing healthcare systems. Establishing a standard for quality assurance facilitates the incorporation of advanced technologies into standard medical practice, benefitting both patients and healthcare practitioners.

The gamma camera system satisfies all performance standards according to the test findings. The system's homogeneity, spatial resolution, sensitivity, and head registration have been confirmed to operate within acceptable parameters, guaranteeing its preparedness for clinical use. This improved performance will allow the system to consistently provide high-quality diagnostic images, assisting the clinical team in providing precise diagnoses and successful treatment strategies.

Author declarations

Funding statement

This research received no specific grant from any funding agency in the public, commercial, or not-for-profit sectors.

Conflict of interest declaration

The authors declare that they have no known competing financial interests or personal relationships that could have appeared to influence the work reported in this paper.

References

1. Gutfilen B, Valentini G. Radiopharmaceuticals in nuclear medicine: Recent developments for SPECT and PET studies. *Biomed Res Int.* 2014; 32: 426892-3.

2. Yang F, Yang K, Yang C. Development and application of gamma camera in the field of nuclear medicine. *Int J Sci.* 2018; 7: 21-24.
3. Wheat JM. An introduction to nuclear medicine. *Australian Institute of Radiography.* 2011;58(3):38-45.
4. Bolstad R, Brown J, Grantham V. Extrinsic versus intrinsic uniformity correction for γ -cameras. *J Nucl Med Technol.* 2011; 39: 208-212.
5. Polito C, Pani R, Frantellizzi V, et al. Imaging performances of a small FoV gamma camera based on CRY018 scintillation crystal. *Nucl Instrum Methods Phys Res A.* 2018; 912: 33-35.
6. Imbert L, Poussier S, Franken PR, et al. Compared performance of high-sensitivity cameras dedicated to myocardial perfusion SPECT: A comprehensive analysis of phantom and human images. *J Nucl Med.* 2012; 53: 1897-1903.
7. Soni PS. Quality control of imaging devices. *International Atomic Energy Agency (IAEA).* 1992; 49-87.
8. Moreno AM, Laguna RA, Trujillo ZFE. Implementation of test for quality assurance in nuclear medicine gamma camera. *United States.* 2012.
9. White S. Gamma camera and SPECT routine quality assurance testing. *Med Phys.* 2010; 37: 3377-3377.
10. International Atomic Energy Agency (IAEA). *Quality assurance for SPECT systems, human health series No. 6.* Vienna: IAEA. 2009.
11. NEMA Standard Publication NU 1. *Performance Measurements of Scintillation Cameras. Radionuclide imaging, EC Standard 61675-2.* *J Med Phys Appl Sci.* 2022; 7: 22.
12. Murphy PH. Acceptance testing and quality control of gamma cameras, including SPECT. *J Nucl Med.* 1987; 28: 1221-1227.
13. Abu Al Roos NJ. Review on routine quality control procedures in nuclear medicine instrumentation. *J Eng Sci Technol.* 2020; 1-5.
14. Aida A, Prajitno P, Soejoko DS. Comparison of SPECT quick QC between using in-house hot phantom and Jaszczak phantom: A preliminary study. *J Phys Conf Ser.* 2019; 1248: p012034.
15. Vaiano A. *Standard operating procedures for quality control of gamma cameras.* Cham: Springer International Publishing. 2019.
16. Sokole BE, Płachcińska A, Britten A. Acceptance testing for nuclear medicine instrumentation. *Eur J Nucl Med Mol Imaging.* 2010; 37: 672-681.
17. Macey DJ. The uniformity of gamma cameras. *Phys Med Biol.* 1972; 17: 857-858.
18. Elkamhawy AA, Rothenbach JR, Damaraju S, Badruddin SM. Intrinsic uniformity and relative sensitivity quality control tests for single-head Gamma cameras. *J Nucl Med Technol.* 2000; 28: 252-256.
19. Abdullah MNA. Intrinsic uniformity test for a dual-head SPECT gamma camera. *Bangladesh J Phys.* 2013; 13: 19.
20. Edam N, Fornasier MR, Denaro MD, et al. Quality control in dual head gamma-cameras: Comparison between methods and software used for image analysis. *Appl Radiat Isot.* 2018; 141: 288-291.
21. International Atomic Energy Agency. *Nuclear medicine physics.* Vienna: IAEA. 2015.